Carbohydrate Polymers 83 (2011) 1345–1354

Contents lists available at ScienceDirect

Carbohydrate Polymers

journal homepage: www.elsevier.com/locate/carbpol

Biodegradable pH-responsive alginate-poly (lactic-co-glycolic acid) nano/micro hydrogel matrices for oral delivery of silymarin

Ibrahim M. El-Sherbiny[a,c], Mamdouh Abdel-Mogib[b], Abdel-Aziz M. Dawidar[b], Ahmed Elsayed[b], Hugh D.C. Smyth[c,*]

[a] Polymer Laboratory, Chemistry Department, Faculty of Science, Mansoura University, ET-35516 Mansoura, Egypt
[b] Natural Products Laboratory, Chemistry Department, Faculty of Science, Mansoura University, ET-35516 Mansoura, Egypt
[c] Division of Pharmaceutics, College of Pharmacy, The University of Texas at Austin, Austin, TX 78712, USA

ARTICLE INFO

Article history:
Received 26 July 2010
Received in revised form
17 September 2010
Accepted 24 September 2010
Available online 8 October 2010

Keywords:
Alginate
Nanoparticles
Silymarin
Oral drug delivery
Hydrogels

ABSTRACT

This study involves the development and characterization of a series of sodium alginate-based pH-responsive hydrogel microspheres encapsulating poly(D,L-lactic-co-glycolic acid) (PLGA) nanoparticles (NPs). The effect of the drying technique (air- or freeze-drying) on the size of the developed particles was determined. Swelling characteristics at different pH values, *in vitro* biodegradation and moisture contents of both air-dried and freeze-dried hydrogel particles were investigated. The effect of drying method on the morphology of the particles was also studied using SEM and AFM. Then, the developed alginate-PLGA particles were evaluated as potential carriers, through a new approach, to improve the dissolution, bioavailability and oral sustained release of silymarin, as a model of hydrophobic natural therapeutics. The used silymarin was isolated from the seeds of some native milk thistle (*Silybum marianum*) ecotypes of delta Egypt and was characterized with the aid of several analytical techniques including; ^{1}H NMR, UV and FTIR. The obtained data showed a considerable effect of the alginate content and the drying method onto the characteristics of the prepared particles. Also, the results demonstrated that the developed alginate-based hydrogel microparticles encapsulating silymarin-loaded PLGA NPs can be used as biodegradable carriers that can confer sustained oral release of silymarin in addition to enhancing its overall dissolution and oral bioavailability.

1. Introduction

Sodium alginate, a non-toxic biodegradable polyanionic copolymer, consists of 1,4-linked β-D-mannuronic acid (M) and α-L-guluronic acid (G) residues arranged either as consecutive blocks or in a random distribution. Alginate has a distinctive ability to form hydrogels via ionotropic crosslinking in presence of divalent cations such as calcium and barium ions (Murata et al., 2009). The hydrogels based on calcium-crosslinked alginate have been widely investigated for various drug delivery purposes (El-Sherbiny, 2010; El-Sherbiny et al., 2010; Murata et al., 2009; Zahoor et al., 2005). However, some reported studies showed relatively rapid drug release rates from the alginate matrices (Chan and Heng, 2002). On the other hand, poly (D,L-lactic-co-glycolic) acid (PLGA) particles showed a very slowly drug release (Jain, 2000). Hence, there had been a few investigations on the use of alginates in combination with PLGA for drug delivery either as composites (Liu et al., 2006) or through coating process (Liu et al., 2004).

This current contribution involves the development and characterization of a series of sodium alginate-based pH-responsive hydrogel microspheres encapsulating PLGA nanoparticles (NPs). These alginate-PLGA matrices were then assessed as potential carriers, through a new approach, to improve the dissolution, bioavailability and oral sustained release of silymarin as a model of natural therapeutics.

Silymarin, a mixture of mainly three flavonolignans (silybin, silychristin and silydianin), is extracted from the milk thistle. The milk thistle, *Silybum marianum* (L.) Gaernt, a member of the *Asteraceae* family, is an herb whose fruits have been used medicinally for more than two millennia (Morazzoni and Bombardelli, 1995). A large number of *in vitro* and *in vivo* studies have confirmed the antioxidant activity of silymarin (Beckmann-Knopp et al., 2000; Sheu et al., 1998) and its ability to encourage protein synthesis and cell regeneration (Sonnenbichler and Zetl, 1986; Sonnenbichler et al., 1999). Also, silymarin was found clinically successful in the treatment of various liver diseases such as acute and chronic viral hepatitis, toxin-induced hepatitis and cirrhosis, and alcoholic liver disease (Flora et al., 1998; Luper, 1998; O'Hara et al.,

* Corresponding author at: Division of Pharmaceutics, College of Pharmacy, The University of Texas at Austin, Austin, TX 78712, USA. Tel.: +1 512 471 3383.
E-mail address: Hsmyth@mail.utexas.edu (H.D.C. Smyth).

0144-8617/$ – see front matter © 2010 Elsevier Ltd. All rights reserved.
doi:10.1016/j.carbpol.2010.09.055

Table 1
The spectral data of silybin, the main bioactive isolate of silymarin, extracted in the study.

^{1}H NMR		
H atom	Chemical shift, δ (ppm)	J (Hz)
2	5.06 (d, 1H)	11.4
3	4.63 (d, 1H)	11.4
6	5.94 (d, 1H)	2.3
8	5.93 (d, 1H)	2.3
2′	7.06 (d, 1H)	2.3
5′	6.86 (d, 1H)	8.4
6′	7.05 (d, 1H)	8.3
α	4.14 (m, 1H)	–
β	4.97 (d, 1H)	8.4
γ	3.47 (d, 1H)	7.6
	3.50 (d, 1H)	10.7
2″	6.93 (dd, 1H)	6.1, 2.3
5″	6.84 (d, 1H)	8.4
6″	6.94 (dd, 1H)	8.4, 2.3
5-OH	11.68 (s, 1H)	–
–OCH_3	3.77 (s, 3H)	–

UV absorption	
λ (nm)	Absorbance
224	0.866
244	0.695
306	0.549
358	0.145

FTIR
υ_{max} (cm^{-1})
3409
2933, 1739
1639
1513, 1464
1363, 1275
1160, 1085
1027, 995
823, 786
638

1998; Pepping, 1999). In addition, it was reported that silymarin inhibits carcinogenesis and, for this reason, it has been used effectively in the treatment of certain types of cancers including skin, breast and prostate (Zi, Feyes, et al., 1998; Zi, Grasso, et al., 1998; Lahiri-Chatterjee et al., 1999). Moreover, silymarin showed antidiabetic (Matsuda et al., 2005), hypolipidaemic, anti-inflammatory (Jeong et al., 2005; Jia et al., 2001; Kang et al., 2004), cardioprotective, neurotrophic and neuroprotective effects. Silymarin has also found potential applications in anti-ageing formulations (Baumann, 2005; Bombardelli et al., 1991).

In spite of the wide range of superior medicinal characteristics of silymarin, its therapeutic efficacy in humans is very limited due to its poor water solubility and low bioavailability after oral administration (Pepping, 1999). Several approaches have been applied to enhance the dissolution and bioavailability of silymarin. These include incorporating silymarin into solid dispersion (Chen et al., 2005), forming a complex based on silymarin and phosphatidylcholine (Barzaghi et al., 1990; Schandalik et al., 1992) and recently via using lipid-based self-microemulsifying drug delivery systems (SMEDDS) (Wu et al., 2006). However, to date, there are no reported studies that enhanced the bioavailability of silymarin via incorporating into a polymeric matrix. Incorporation of silymarin in polymeric nano-carriers might be advantageous over other carriers such as lipid-based systems because of relative stability, increased water solubility, improved permeability across the physiological barriers, considerable changes in drug biodistribution, increased bioavailability and also reduction of undesirable side effects (Trubetskoy, 1999). In addition, the polymeric nano-carriers can be designed to show desirable physico-chemical characteristics via the well selection of appropriate candidates from a wide range of natural and synthetic polymers. Therefore, in this study, silymarin-loaded PLGA NPs were synthesized using "single emulsion-solvent evaporation technique" through a modified procedure. The suspensions of these silymarin-loaded PLGA NPs in aqueous sodium alginate solutions were then employed to produce pH-sensitive hydrogel microparticles via the ionotropic crosslinking in mild aqueous medium. The resulting alginate-PLGA hydrogel particles were characterized and evaluated as new biodegradable carriers that can enhance the dissolution and oral bioavailability of silymarin and at the same time confer sustained oral release of the drug.

2. Experimental

2.1. Materials

Plant material: *Silybum marianum* (*Asteraceae*) was collected from south Mansoura city, Egypt in June 2007 and identified by Division of Plant Ecology, Botany Department, Faculty of Science, Mansoura University, Egypt. Chemicals: Poly(D,L-lactic-co-glycolic acid) (PLGA) copolymer with 50/50 molar composition of lactic/glycolic acid and with an inherent viscosity of 0.15–0.25 dl/g, sodium alginate (low viscosity; 250 cps for a 2% solution at 25 °C) and polyvinyl alcohol (PVA), MW 12–23 kDa, 87–89% hydrolyzed, were supplied by Sigma–Aldrich (St. Louis, MO, USA). Methylene chloride was purchased from Fisher Scientific (Fairlawn, NJ, USA). The solvents; petroleum ether (60–80), hexane, diethyl ether, chloroform, ethyl acetate, acetone, ethanol and methanol were obtained from Adwic Company (Cairo, Egypt). Phosphate buffer saline solutions and all other reagents were of analytical grade and used as received.

2.2. Methods

2.2.1. Processing of the plant material

In a 2 L conical flask, ground *Sylbum marianum* seeds (400 g) were mixed with 1200 ml of petroleum ether. The obtained suspension was then refluxed with stirring for 30 min and further stirred for additional 5 h. Afterwards, the herbal material was vacuum filtered using a Buchner funnel and the remaining seed residue was further washed with petroleum ether (2 × 100 ml). The filtrate was then evaporated to give a clear yellow-orange oil of weak characteristic scent (75 g, about 19%, based on weight of the crude seeds). The defatted *Sylbum marianum* seeds (approx. 325 g) were mixed in 2 L conical flask with 1200 ml of acetone and stirred at room temperature for 96 h. The suspended herbal material was vacuum-filtered using a Buchner funnel. After removal of the acetone, about 33 g of the dry extract was obtained as yellow-orange crystals mottled with yellow-orange oil. Then, 50 ml of diethyl ether was added and stirred while heating to the solvent refluxed temperature for about 60 min, after which the suspension was allowed to cool down to the room temperature. The resulting crystals were filtered and washed with 2 × 25 ml portions of cold diethyl ether and the product was air-dried. Silymarin, in form of small shiny crystals, with a color ranging from yellow to light orange, was obtained (11 g, about 2.7% based on the initial weight of the crude seeds). The obtained silymarin mixture melts slowly from 140 to 165 °C.

2.2.2. Characterization

^{1}H NMR spectra were recorded on a 500 MHz spectrometer (JEOLl, USA). Chemical shifts are given in ppm relative to TMS as internal standard. Infrared spectra were carried out for a thin film

Table 2
The composition of the developed hydrogel microparticles encapsulating silymarin-loaded PLGA NPs and some of their characteristics.

Sample code	SA[a] (W%)	PLGA NPs (W%)	$CaCl_2$ [M]	Geometric size[b] (μm)		LE% ± SD[c]	Feret's diameter[d] (μm)		Sieve diameter (μm)		Moisture content (%)	
				FD	AD		FD	AD	FD	AD	FD	AD
F1	100	00	0.2	985 ± 7	–	71.4 ± 4	1015 ± 105	–	817 ± 83	–	10.8	1.6
F2	90	10	0.2	1328 ± 107	946 ± 12	80.0 ± 3	1322 ± 156	1126 ± 167	825 ± 158	892 ± 146	10.4	1.8
F3	80	20	0.2	1348 ± 63	1052 ± 45	75.1 ± 2	1520 ± 96	1208 ± 109	1226 ± 117	990 ± 101	15.7	1.1
F4	65	35	0.2	1760 ± 112	–	77.3 ± 5	1918 ± 193	–	1287 ± 206	–	17.1	2.5
F5	50	50	0.2	1496 ± 108	–	88.7 ± 2	1603 ± 286	–	1038 ± 113	–	22.1	4.1

[a] Sodium alginate.
[b] Geometric size as determined using digital caliber.
[c] Loading efficiency.
[d] As determined using ImageJ software (NIH).

casted from $CHCl_3$, and performed on a Mattson 5000 FTIR spectrometer. The thin layer chromatography and the preparative TLC were performed on silica gel (Kieselgel 60, GF 254) of 0.25 mm thickness. The spectral data of the isolated silybin, the main active component in silymarin, are summarized in Table 1.

2.2.3. Preparation of silymarin-loaded PLGA NPs

The silymarin-loaded PLGA NPs were prepared using "single emulsion-solvent evaporation technique" through a procedure similar to that described in the literature (Cartiera et al., 2010). Briefly, PLGA (250 mg) was dissolved in 10 ml of methylene chloride. To this PLGA solution, a 50 mg of the pure extracted silymarin dissolved in 5 ml of ethanol was added with stirring. A 3% w/v aqueous PVA solution (15 ml) was prepared to which, the PLGA/silymarin mixture was added dropwise while vortexing the surfactant (PVA) solution at a high setting. Then the entire contents were sonicated for 2 min at 45% amplitude with a probe type sonicator (Misonix ultrasonic processor, S-4000, Misonix Inc, CT, USA) to create an oil-in-water emulsion. The sonication step was repeated three times until the desired size was obtained. Sonication was performed in an ice-water bath with applying pulse function (pulse on 5 s and pulse off 5 s) in order to avoid the heat built-up of the polymer/silymarin solution during the sonication. After sonication, the emulsion was immediately poured into 50 ml of an aqueous 0.3% w/v PVA solution under rapid stirring with a magnetic stirrer. The resulting nano-sized PLGA emulsion was stirred overnight in uncovered container to allow for ethanol and methylene chloride evaporation. The resulting PLGA NPs suspension was completed to 100 ml volume with de-ionized water and further used in the preparation of the pH-responsive hydrogel microparticles.

2.2.4. Preparation of the alginate-PLGA hydrogel microparticles

A series of hydrogel matrices were developed via ionotropic gelation of sodium alginate solution containing silymarin-loaded PLGA NPs using calcium chloride solution as the coagulation fluid. In brief, a predetermined volume of silymarin-loaded PLGA NPs suspension obtained in the previous section was added dropwise with homogenization (4000 rpm) to a calculated volume of 3% aqueous alginate solution (Table 2). The polymer mixture was then diluted with distilled water until obtaining same final concentration (1.5% w/v) in all the prepared formulations. The homogenized polymer mixtures were then dropped into 75 ml of gently stirred (200 rpm) calcium chloride solution (0.2 M) through a 10 ml syringe with a 21 gauge needle at a dropping rate of 1.5 ml/min. The formed particles were allowed to crosslink with the Ca^{2+} in solution for 15 min. The resulting calcium-crosslinked microparticles were collected and washed with distilled water (25 ml) to remove the unreacted calcium chloride. A fraction of each microparticle formulation was freeze dried while the remaining amount was left in a Petri dish to dry in air at room temperature. Both freeze-dried and air-dried hydrogel microparticles were then stored until further use. The composition of the four developed formulations (F2–F5) in addition to a control formulation based on alginate alone (F1) are given in Table 2.

Both the $CaCl_2$ solution (75 ml), used in each experiment, and the washings (25 ml) were collected and filtered. Then, their content of silymarin was estimated from the absorption at λ_{max} 325 nm with aid of UV–Vis spectrophotometry (Infinite M 200 fluorophotometer, TECAN, USA). The difference between the amount of silymarin initially loaded and that estimated in the 100 ml (washings plus $CaCl_2$) was taken as a measure of the actual amount of silymarin entrapped. The mean values for three replicate determinations and their mean ± SD values were reported. The loading efficiency (L.E.%) of silymarin was calculated as follows:

$$\text{L.E.\%} = \left(\frac{m_r}{m_i}\right) \times 100 \quad (1)$$

where m_i and m_r are the amounts (mg) of the silymarin initially loaded and remained in the developed hydrogel microparticles, respectively.

2.2.5. Determination of particle size

The size of the prepared silymarin-loaded PLGA NPs was determined by Dynamic light scattering, DLS (Malvern nano-sizer, Malvern Instruments Ltd., Worcestershire, UK). The average geometric diameters of the developed hydrogel microparticles were measured using a digital caliber (General® Ultra-Tech). In addition, the average sieve and Feret's diameters of the hydrogel microparticles were determined by light microscopy with aid of ImageJ software (NIH). The diameters were determined as the mean values of 10 randomly selected microspheres (n = 10).

2.2.6. Surface morphology analysis

The surface morphology of the hydrogel microparticles was examined by SEM (Zeiss supra 40 VP scanning electron microscope). Dry particles were mounted on aluminum stubs with double-sided conducting carbon tapes and coated with a 50/50 mixture of Pt/Pd to minimize surface charging. The samples were scanned at an accelerating voltage of 20 kV. The surface morphology of the developed hydrogel microparticles encapsulating PLGA NPs was also examined using atomic force microscopy, AFM (Multimode scanning probe atomic force microscope, Veeco Instruments, USA).

2.2.7. Moisture content determination

The moisture content of the hydrogel microparticles encapsulating PLGA NPs was determined using HR83 Halogen Moisture Analyzer (Mettler-Toledo GmbH, Switzerland). A sample of 250–300 mg was heated at 115 °C for 3 min. The content of moisture in the samples was obtained as the percentage of weight loss. The obtained values were the mean ± SD from three independent determinations.

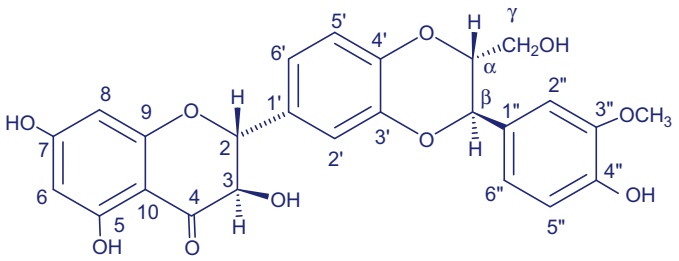

Fig. 1. Chemical structure of the main bioactive silymarin isolate (silybin).

2.2.8. Swelling characteristics

The equilibrium swelling values of the hydrogel matrices were determined by incubating a pre-weighed sample in 15 ml buffer solution of pH 2.1 (SGF) or pH 7.4 (SIF) at 37 °C with shaking (100 rpm) until attaining the equilibrium. The swollen samples were then weighed after removing the surface water. The dynamic swelling patterns of both freeze-dried and air-dried hydrogel microparticles were also determined. Briefly, a certain weight of the dried hydrogel microparticles was incubated at 37°C with shaking (100 rpm) in 15 ml buffer of either pH 2.1 or pH 7.4 for 24 h. Swollen weights of the hydrogel microparticles were determined at intervals, after blotting surface liquid. The swelling % of the hydrogel formulations was then calculated using the following relationship:

$$S(\%) = \frac{W_t - W_o}{W_o} \times 100 \quad (2)$$

where W_o is the initial weight and W_t is the final weight of the swollen hydrogel microparticles at time t. The data points represent the average ± SD from three independent swelling experiments.

2.2.9. Biodegradation study

The biodegradation of the prepared hydrogel matrices was carried out in presence of 0.2% lysozyme dissolved in PBS, pH 7.4 (Hirano et al., 1989). In a typical procedure, pre-weighed samples (50–100 mg) were transferred to small vials and incubated with 5 ml of lysozyme solution at 37 °C with shaking (100 rpm) for 2 h until the hydrogel microparticles almost attained equilibrium swelling. The weights of swollen samples (m_o) were determined after decanting the solvent. Then, 5 ml of fresh lysozyme solution was added to the swollen microparticles. At different intervals starting from determination of m_o, the steps of solvent decantation and weighing were repeated and the final weights (m_t) at these intervals were recorded. The biodegradation of the developed hydrogel microparticles was determined as the percentage of weight loss (W_d %) of samples due to enzymatic degradation as in the following relationship:

$$W_d(\%) = \frac{m_o - m_t}{m_o} \times 100 \quad (3)$$

where m_o is the weight of sample after 2 h swelling in lysozyme solution and m_t is the weight of sample after incubation with lysozyme for a given time t.

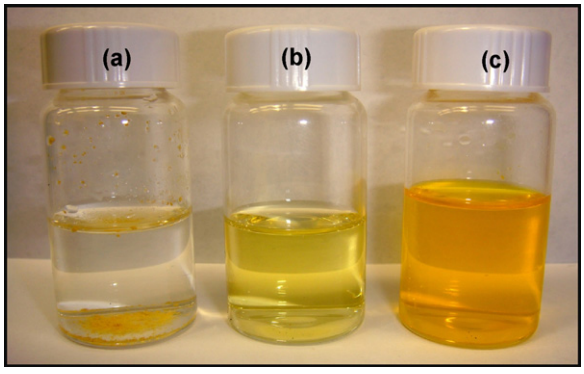

Fig. 2. Photographs showing: (a) silymarin suspended in distilled water, (b) silymarin solution in ethanol and (c) aqueous suspension of silymarin-loaded PLGA NPs.

2.2.10. In vitro release study of silymarin

The *in vitro* cumulative release profiles of the loaded silymarin were determined by incubating pre-weighed hydrogel microparticles encapsulating silymarin-loaded PLGA NPs in 10 ml buffer of pH 2.1 (SGF) at 37 °C with shaking (100 rpm) for 3 h and subsequently in 10 ml of pH 7.4 (SIF) at 37 °C. At intervals, 100 μl aliquot was withdrawn and analyzed at λ_{max} 325 nm using a UV–Vis spectrophotometer (Infinite M 200 fluorophotometer, TECAN, USA). Each time, the withdrawn sample was replaced with an equal volume of fresh buffer, to keep the volume of the release medium constant. The release data points represent mean ± SD from three independent experiments.

2.2.11. Statistical analysis

The data was analyzed and expressed as mean ± SD from three independent experiments. The effect of various parameters on the characteristics of the developed hydrogel microparticles encapsulating PLGA NPs were statistically analyzed by one-way ANOVA (Microsoft Excel 2007). The differences were considered significant at the level of $P < 0.05$.

3. Results and discussion

3.1. Isolation of silymarin and its spectral characteristics

Milk thistle (*Silybum marianum* L. Gaertner, Asteraceae), an herbaceous annual or biennial plant, is native to the Mediterranean region, however, it has been naturalized by cultivation in the dry and hot regions of Africa, southern Europe, China, South America, some parts of North America and Australia (Morazzoni and Bombardelli, 1995). Silymarin, a mixture of mainly three flavonolignans (silybin, silychristin and silydianin) that is extracted from the milk thistle, has found to be good antioxidant with a superior hepatoprotector and anticancer activity plus many other pharmacological activities (Zi et al., 1998a; Pepping, 1999). The therapeutic characteristics of silymarin have been attributed specifically to the presence of silybin as the most active isolate in silymarin (represents about 60%), (Wu et al., 2006). The chemical structure of silybin is illustrated in Fig. 1.

The silymarin content in the milk thistle depends mainly on the geographic and climatic conditions in which these plants grow. The silymarin used in this study was isolated from the seeds of some native milk thistle ecotypes of delta Egypt. Silymarin isolation was achieved by a two-steps (defatting and extraction) process according to Kim et al. (2003). The resulting silymarin samples were analyzed with aid of several analytical and spectral equipments include ^{1}H NMR, UV and FTIR. The spectral data of the silybin, as the most important bioactive isolate of silymarin and as example for other isolated components, were summarized in Table 1. The spectral data of all the silymarin components, including silybin, extracted in the current study were found to be in agreement with those reported in literature by Kim et al. (2003).

3.2. Preparation of the alginate-PLGA hydrogel matrices

Silymarin-loaded PLGA NPs were prepared using "single emulsion-solvent evaporation" method through a procedure similar to that described by Cartiera et al. (2010). This preparation

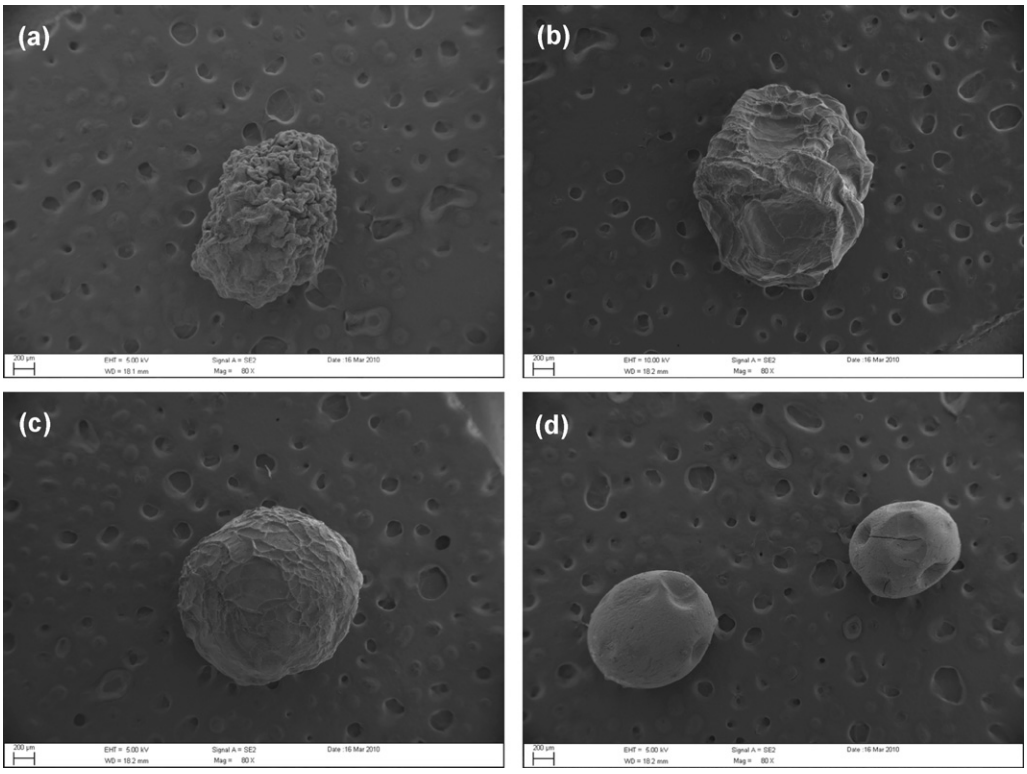

Fig. 3. Scanning electron micrographs of the freeze-dried hydrogel microparticles (a) F1, (b) F2, (c) F3 and (d) the air-dried F3.

technique is ideal for encapsulation of hydrophobic ingredients such as silymarin. Also, the encapsulation of the water-insoluble silymarin into nano-sized particles would enhance the dissolution and consequently the bioavailability of silymarin. This beneficial role played by nanoencapsulation is illustrated in Fig. 2. From the figure, the silymarin solubility in water is very limited (maximum, 0.5 mg/ml at 25 °C, Fig. 2a) as compared to those in some organic solvents such as ethanol (Fig. 2b). Fig. 2c shows the aqueous suspension of the silymarin-loaded PLGA NPs. Nanoencapsulation of the silymarin led to a stable colloidal dispersion with strong color, indicating the homogenous distribution of silymarin in the aqueous medium at a significantly higher concentration (290 mg/ml) than that obtained using solvents (215 mg/ml ethanol). This would improve the extent of silymarin absorption (bioavailability) in the gastrointestinal tract.

The prepared silymarin-loaded PLGA NPs were incorporated into a calcium-crosslinked alginate matrix to develop a series of biodegradable pH-responsive hydrogel microparticles (Scheme 1). Encapsulation of the silymarin-loaded PLGA NPs into these alginate-based pH-responsive hydrogels allows a sustained release of the silymarin and silymarin-loaded PLGA NPs particularly in the intestinal region.

3.3. Microparticle surface morphology study

Fig. 3 shows the scanning electron micrographs for some freeze-dried and air-dried alginate hydrogel microparticles encapsulating silymarin-loaded PLGA NPs. From the figure, the freeze-dried microparticles containing PLGA NPs (Fig. 3b and c) are, in general, more spherical and regular than those prepared from alginate alone (Fig. 3a). Comparing the micrographs of freeze-dried F2 microparticles (Fig. 3b) with that of F3 microparticles (Fig. 3c) shows that increasing the content of PLGA NPs tended to increase the particles regularity and they tended to have more dense and integrated surfaces. The figure also reveals the effect of drying method on the particle regularity and surface morphology. For instance, the air-dried F3 microparticles (Fig. 3d) appear more compact, dense, relatively smaller, and smoother than those F3 microparticles obtained via freeze-drying (Fig. 3c).

The surface morphology of developed alginate hydrogel microparticles encapsulating PLGA NPs can be seen more clearly in Fig. 4. As apparent from the figure, the freeze-dried hydrogel microparticles prepared from alginate alone, F1 (Fig. 4a) showed a highly folded surface (very high rugosity). Conversely, both air-dried F2 and F3 hydrogel microparticles (Fig. 4b and c) exhibit more compact and relatively smoother surfaces. In addition, evidence of the encapsulated silymarin-loaded PLGA NPs can be observed on the surface of the developed hydrogel microparticles (Fig. 4b and c). These encapsulated silymarin-loaded PLGA NPs appear spherical and of appropriate sizes. The encapsulated silymarin-loaded PLGA NPs can also be seen clearly in the AFM image (Fig. 5) of the surface of the prepared hydrogel microparticles.

3.4. Particle size

The diameter of the synthesized silymarin-loaded PLGA NPs was found to be 266 ± 41 nm as determined by DLS. This size of the synthesized silymarin-loaded PLGA NPs was confirmed by the results of both SEM (Fig. 4b and c) and AFM (Fig. 5). With the aid of AFM particle analysis software (NanoScope Analysis, Veeco Co, USA), the average diameter of these silymarin-loaded PLGA NPs was found to be 258 ± 34 nm. In case of the hydrogel microparticles encapsulating PLGA NPs, their average geometric diameters were found to be in the range of 946 ± 12 to 1760 ± 112 μm as determined using a digital caliber (General® Ultra-Tech). From the size data in Table 2, it is obvious that geometric diameters of the freeze-dried hydrogel microparticles are statistically larger than that of the air-dried microparticles. For instance, the geometric diameters of the freeze-dried F2 and F3 microparticles are 1328 ± 107 μm and 1348 ± 63 μm whereas, the diameters of the correspond-

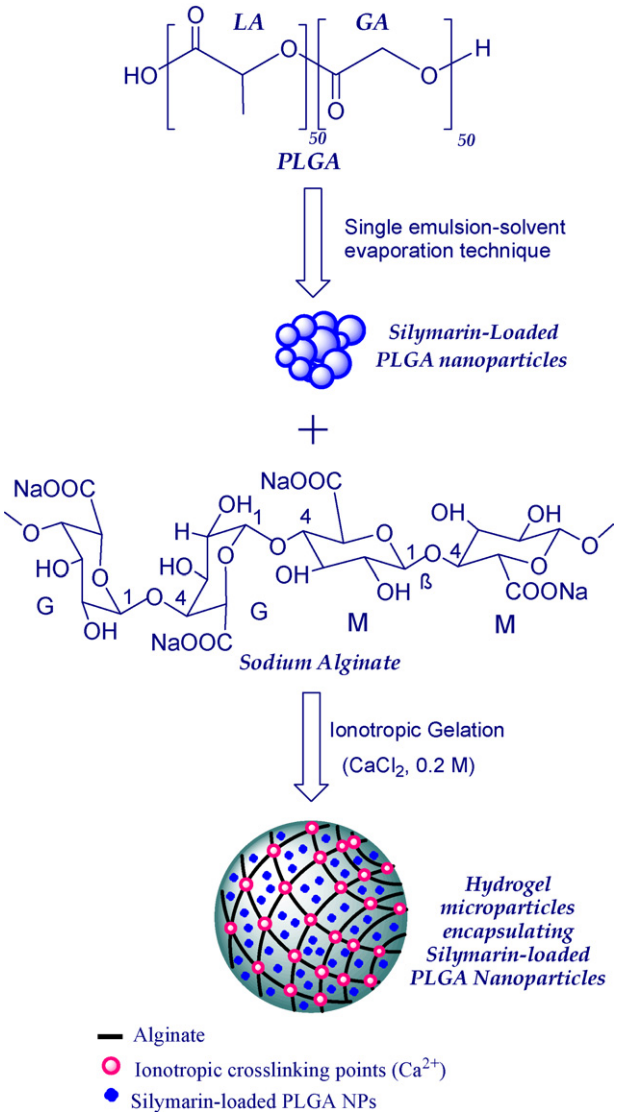

Scheme 1. A schematic illustration for the preparation of the hydrogel microparticles encapsulating silymarin-loaded PLGA NPs.

ing air-dried microparticles are 946 ± 12 μm and 1052 ± 45 μm, respectively. It seems also that the microparticles formulations encapsulating PLGA NPs have relatively larger sizes as compared to those developed from alginate alone (F1). In the formulations containing PLGA NPs (F2–F5), increasing the alginate content relative to that of the encapsulated PLGA NPs tends to decrease the particle size. This reduction in size may be attributed to increasing the available calcium–alginate crosslinking extent of the microparticles as the alginate percent increases. For instance, the diameters of freeze-dried F4 (65% alginate), F3 (80% alginate) and F2 (90% alginate) are 1760 ± 112, 1348 ± 63 and 1328 ± 107 μm, respectively. In addition, both Feret's and sieve diameters of the developed hydrogel microparticles were measured with aid of ImageJ software (NIH). In general, Feret's diameter represents the measured distance between two tangents on opposite sides of the particle while, sieve (inner) diameter is the diameter of the maximum inscribed circle (the maximum circle lying completely inside the particle) (Ortega-Rivas, 2005). As apparent from the data in Table 2, both Feret's and sieve diameters of the developed hydrogel microparticles attained similar values which can be attributed to the spherical nature of the particles. Moreover, the values of Feret's and sieve diameters recorded in Table 2 confirm the effects of both drying method and

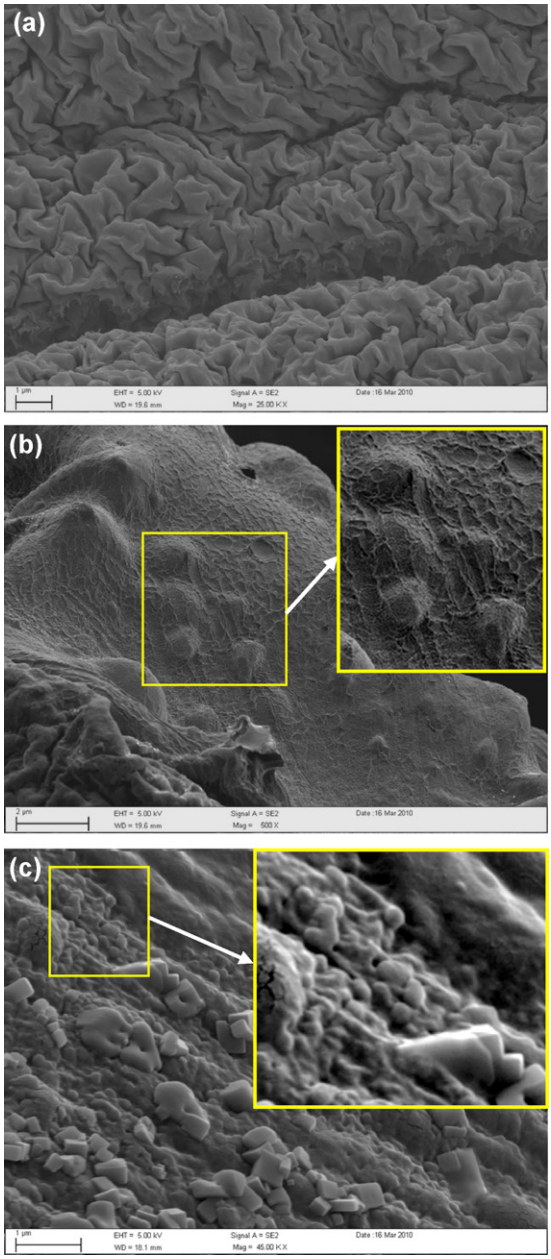

Fig. 4. Surface morphology of (a) freeze-dried F1 hydrogel microparticles, (b) air-dried F2 and (c) air-dried F3 hydrogel microparticles.

alginate content onto the particle size as discussed above for the geometric diameters.

3.5. Moisture content

Table 2 illustrates the moisture content (%) of the freeze-dried and air-dried silymarin-loaded alginate hydrogel microparticles developed in this study. As apparent from the results, the moisture contents of the microparticles fall in the ranges of 10.4–22.1% and 1.1–4.1% for freeze-dried and air-dried microparticles, respectively. It must be noted that these measurements, performed on a moisture balance, involve exposure of the particles to ambient humidity prior to final determination of moisture content. Thus, hygroscopic materials analyzed by this method may appear to have significant moisture content (i.e. freeze-dried samples) due to rapid moisture uptake prior to the measurement. Thus, freeze dried particles not exposed to ambient conditions would be expected to have

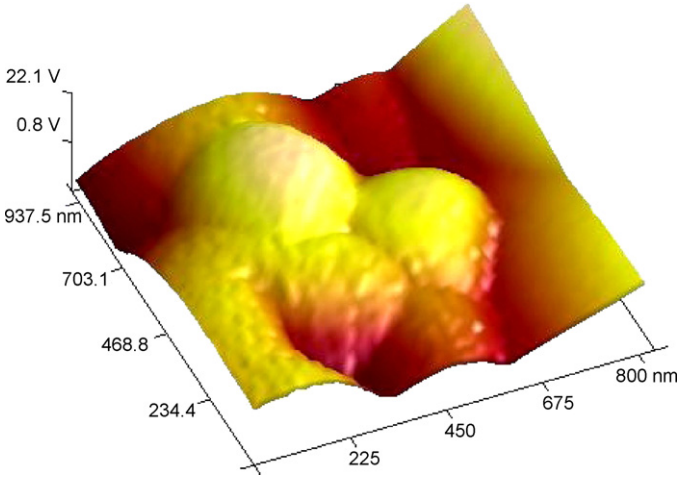

Fig. 5. AFM image of the surface of the developed hydrogel microparticles encapsulating silymarin-loaded PLGA NPs.

lower moisture content than that determined. In general, moisture content of the developed hydrogel microparticles increased with increasing the PLGA NPs content.

3.6. Dynamic swelling study

The swelling patterns of the freeze-dried alginate hydrogel microparticles encapsulating silymarin-loaded PLGA NPs in simulated gastric fluid (SGF, pH 2.1) are shown in Fig. 6. As apparent from the figure, the freeze-dried formulation prepared from alginate alone (F1) achieved significantly ($p < 0.05$) lower swelling values as compared to those containing PLGA NPs. These observations are also supported by the fact that as the percentage of PLGA NPs was increased, equilibrium swelling magnitudes also tended to increase. For instance, F2, F3, F4 and F5 hydrogel formulations attained 331 ± 12, 376 ± 9, 427 ± 6 and 424 ± 9% of swelling at 24 h, respectively. This swelling behavior may be attributed to the

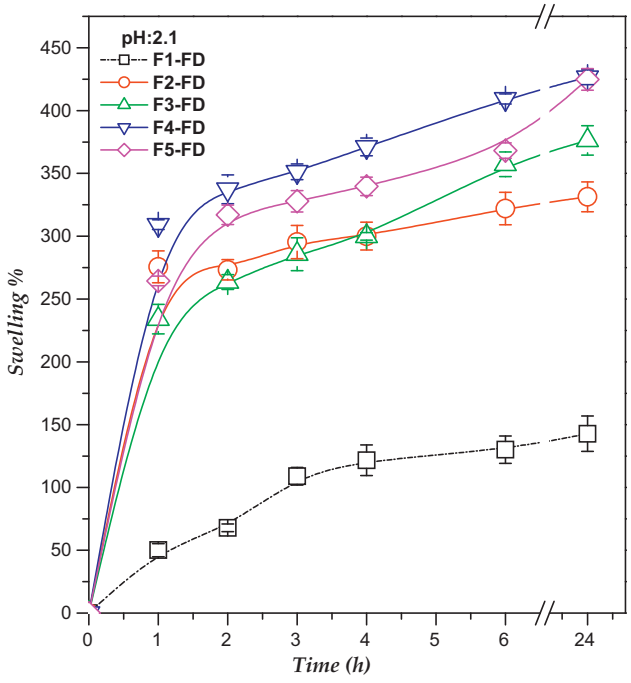

Fig. 6. Swelling patterns of the freeze-dried hydrogel microparticles encapsulating silymarin-loaded PLGA NPs in simulated gastric fluid (SGF, pH 2.1) at 37 °C.

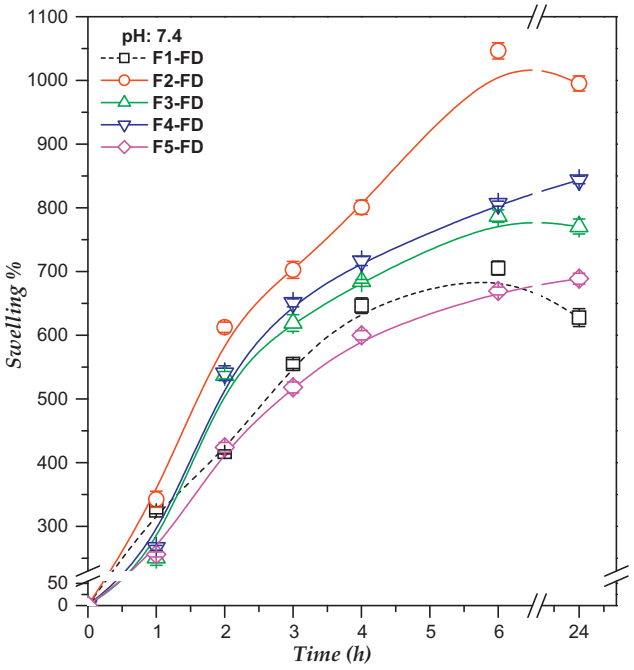

Fig. 7. Swelling patterns of the freeze-dried hydrogel microparticles encapsulating silymarin-loaded PLGA NPs in simulated intestinal fluid (SIF, pH 7.4) at 37 °C.

fact that increasing the content of PLGA NPs within the hydrogel microparticles will lead to a decrease in the crosslinking possibilities of the alginate chains through interaction with calcium ions and consequently increase the swelling values attained at equilibrium. Also, at pH 2.1, the free carboxylate groups of sodium alginate, which are not involved in the ionic crosslinking with Ca^{2+}, will tend to form hydrogen bonds with each other and with the OH groups of the sugar moiety (El-Sherbiny et al., 2010). These hydrogen bonds act to minimize the swelling at pH 2.1 with increasing the alginate content. The role played by the content of PLGA NPs in decreasing the extent of crosslinking and consequently increasing the equilibrium swelling was also confirmed by comparing the swelling profiles of the microparticles formulations containing PLGA NPs (F2–F5) with that of the control, F1 (100% alginate) which attained a swelling value of only 143 ± 14% after 24 h.

Fig. 7 shows the swelling patterns of the freeze-dried hydrogel microparticles encapsulating silymarin-loaded PLGA NPs in a simulated intestinal fluid (SIF, pH 7.4). As shown in the figure, the freeze-dried microparticle formulations containing PLGA NPs (F2–F5) attained relatively higher swelling values at equilibrium as compared to that prepared from alginate alone (F1). This swelling behavior also confirms the suggested role of the PLGA NPs in decreasing the extent of crosslinking and consequently increasing the equilibrium swelling. In case of the hydrogel formulations containing PLGA NPs, increasing the percentage of alginate relative to that of PLGA NPs tended, in general to increase the swelling values attained at equilibrium. For instance, F2 (90% alginate), F3 (80% alginate) and F5 (50% alginate) attained swelling values of 995 ± 12, 771 ± 11 and 689 ± 9%, respectively at 24 h. This is in contrast to the results presented in Fig. 6 for simulated gastric fluid. This behavior can be ascribed to the fact that, at pH 7.4, most of the free carboxylic groups of alginate would be ionized. Consequently, strong repulsive forces are created between these ionized carboxylate groups (COO^-) (El-Sherbiny et al., 2010). These electrostatic repulsion forces are thus responsible for attaining the developed hydrogel microparticles higher values of swelling at pH 7.4 upon increasing the alginate content. From Fig. 7, it can be noted also that some of the hydrogel formulations (such as F1–F3) showed a swelling

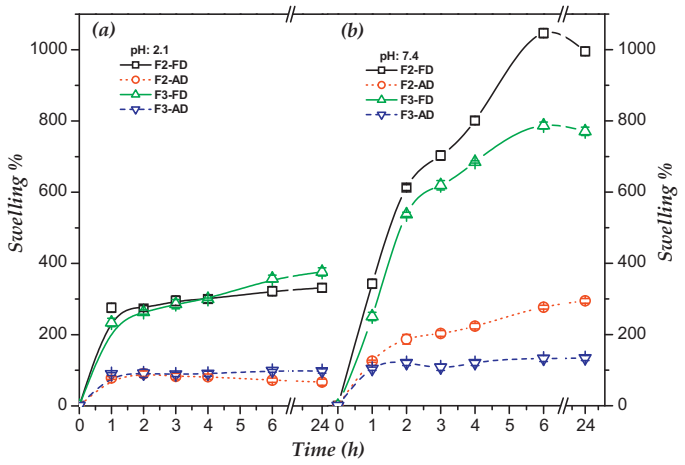

Fig. 8. Swelling patterns of the freeze-dried and air-dried F2 and F3 hydrogel microparticles in simulated gastric and intestinal fluids at 37 °C.

decrease at equilibrium. In general, the fast initial swelling of these hydrogel formulations is due to their highly hydrophilic nature (osmotic driving forces). This is followed by occurrence of a kind of resistance due to the cohesive forces exerted by the crosslinked polymer strands. These cohesive forces tend to resist further hydrogel expansion and encourage some of swelling fluid to be expelled (swelling decrease stage) (Guenet, 1992). The magnitude of these two opposing forces (osmotic and cohesive) depends mainly on the crosslinking density of hydrogels and generally, the equilibrium condition is reached when a balance is achieved between these two forces.

A comparison between the swelling profiles of the freeze-dried and air-dried hydrogel microparticles at both SGF (pH, 2.1) and SIF (pH 7.4) are shown in Fig. 8. As apparent from the figure, at both pHs 2.1 and 7.4, the freeze-dried hydrogel microparticles attained significantly ($p \ll 0.05$) higher swelling values at equilibrium as compared to the air-dried samples. This may be due to the relatively high porosity of the freeze-dried samples as compared to the compact structure of the air-dried microparticles. This porosity in case of the freeze-dried hydrogel samples is attributed in particular to the relatively high speed of solvent removal (sublimation) due to the applied high vacuum whereas, in the case of air-dried samples, the solvent evaporation occurs slowly leading to a more compact structure of the hydrogel matrix. The porosity of the freeze-dried matrices facilitates the entrance of swelling fluid into the hydrogel matrix and consequently attaining higher equilibrium swelling values. These differences in equilibrium swelling between air-dried and freeze-dried microparticles at both pHs, 2.1 and 7.4 can be seen obviously in Fig. 9(b and c).

Fig. 8 also reveals a pH-responsive nature for the developed alginate-based hydrogel matrices. This pH-responsiveness (limited swelling at pH 2.1 and maximum swelling at pH 7.4) is attributed, as described above, to the high crosslinking extent occurred at pH 2.1 due to both ionic interaction with $CaCl_2$ and the H-bonds formation whereas, at pH 7.4, the strong repulsive forces created between the ionized carboxylate groups (COO^-) are the responsible for attaining the hydrogel microparticles higher values of swelling. This pH-responsive characteristic of the developed hydrogels can be observed also in Fig. 9 for both air-dried (Fig. 9b) and freeze-dried (Fig. 9c) microparticles.

3.7. *In vitro* biodegradation study

An *in vitro* biodegradation study of the prepared microparticles encapsulating PLGA NPs was performed in PBS, pH 7.4 in presence of 0.2% (w/v) lysozyme as has been the protocol in previous studies (Hirano et al., 1989). The weight loss percentage of the microparticles as a function of time was determined and taken as a measure of degradation. Fig. 10 reveals the degradation patterns of the hydrogel microparticles. It was found that the degradation extent is significantly ($p < 0.05$) dependent on the method of drying. As apparent from the figure, the freeze-dried microparticles attained higher degradation rates as compared to the air-dried microparticles. For instance, the percentage of degraded weights (W_d %) of the freeze-dried F2 and F3 microparticles are 30.6 ± 2.7 and 37.5 ± 0.3% after 6 days whereas, the corresponding air-dried microparticles attained 14.9 ± 0.9 and 11.5 ± 0.8%, respectively. Similarly to swelling studies, this could be attributed to the porosity of samples formed upon freeze-drying as compared to the more compact and dense structure obtained by air-drying. This porosity will facilitate the diffusion of enzyme through the particle matrix and consequently accelerate degradation. It seems also from the figure that, the freeze-dried formulations prepared from alginate alone (F1) achieved almost the lowest degradation extent as compared to other freeze-dried formulations containing PLGA NPs (F2–F5). In addition, it can be noted from the figure that, decreasing the alginate content in the developed microparticles relative to the content of PLGA NPs tends, in general to increase their degradation rate (high weight loss). This behavior can be attributed to the

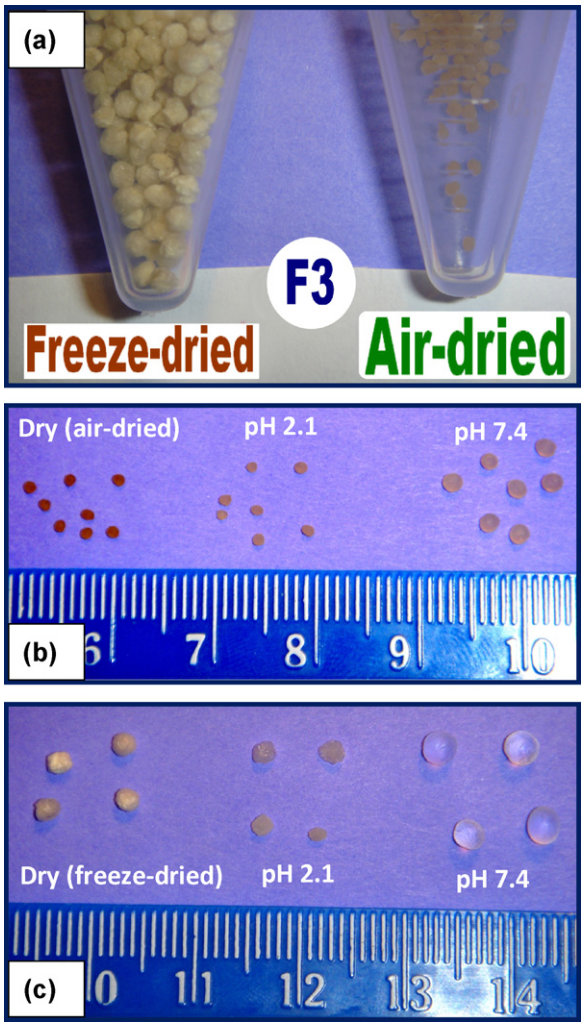

Fig. 9. Photographs of the developed freeze-dried and air-dried F3 microparticles (a), swelled sizes of air-dried F3 microparticles in pHs 2.1 and 7.4 (b) and swelled sizes of freeze-dried F3 microparticles in pHs 2.1 and 7.4 (c).

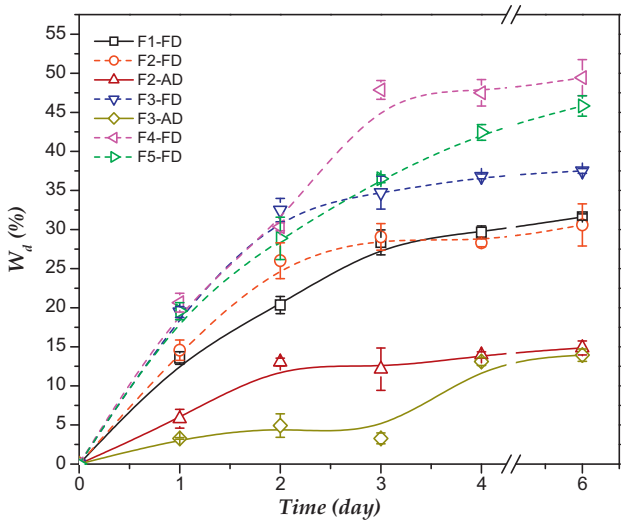

Fig. 10. *In vitro* biodegradation patterns of the developed freeze-dried and air-dried hydrogel microparticles encapsulating silymarin-loaded PLGA NPs in pH 7.4 at 37 °C in presence of 2 mg/ml of lysozyme (W_d %: the percentage of weight loss of samples due to enzymatic degradation).

increase of crosslinking extent upon increasing the alginate content which tends to impede the diffusion of enzyme through the particles and consequently retard their degradation.

3.8. *In vitro* release studies

The loading efficiency (L.E.%) of silymarin in the developed hydrogel microparticles were determined as shown in Table 2. As noted from the table, the estimated L.E.% values are in the range 71.4 ± 4 to 88.7 ± 5. The partial loss of the entrapped silymarin occurs particularly during both the crosslinking process in $CaCl_2$ solution and washing of the resulting hydrogel microparticles after crosslinking. In spite of the general increase in the values of L.E.% with increasing the percent of silymarin-loaded PLGA NPs, the estimated L.E.% values did not follow the anticipated rank order in the formulation F2 which may be attributed to an inefficient washing step of the F2 hydrogel microparticles after the crosslinking process.

The cumulative release profiles of silymarin from the developed alginate-PLGA hydrogel microparticles at 37 °C in both SGF (pH 2.1) and SIF (pH 7.4) are shown in Fig. 11. As apparent from the figure, the percent of silymarin released was much higher in SIF than in SGF because the release rate from a hydrogel is particularly a reflection of its swelling behavior (diffusion mechanism). As discussed earlier, the swelling of the developed microparticles in SIF was much higher than in SGF. In case of freeze-dried microparticles (Fig. 11a), the percent of silymarin released in SIF (pH 7.4) tended, in general, to increase as the alginate content in the microparticles increases. These release patterns of silymarin from the freeze-dried microparticles are in agreement with their swelling behavior in SIF. In SGF (pH 2.1), an agreement can also be noted between the release patterns of silymarin and swelling behavior, though the drug release does not directly follow the rank order of the swelling study.

Fig. 11b reveals the effect of drying method of the microparticles onto the release rates/profiles of silymarin. From the figure, the percent of silymarin released from the freeze-dried microparticles was much higher as compared to that released from the air-dried microparticles in both SGF and SIF. This higher release in case of freeze-dried microparticles could be ascribed to the relatively high porosity of these microparticles as compared to the more dense and compact morphology of the air-dried microparticles.

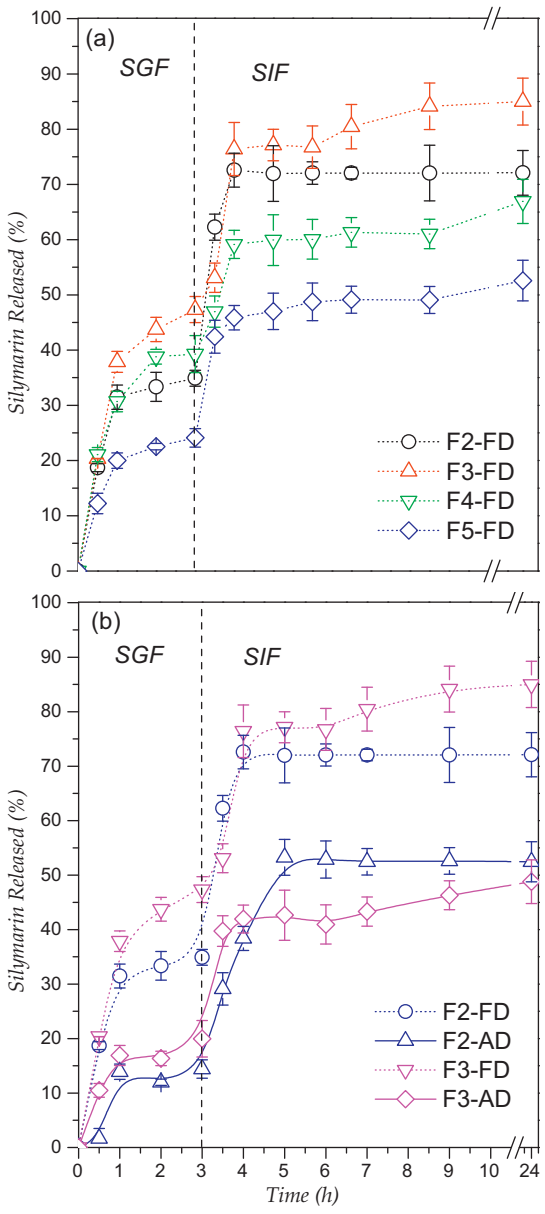

Fig. 11. The release profiles of silymarin from the developed hydrogel microparticles encapsulating PLGA NPs at 37 °C in SGF followed by SIF.

4. Conclusion

This study described a new approach for enhancing the dissolution and oral bioavailability of silymarin as a model of hydrophobic natural therapeutics via formulation in polymeric matrices. These matrices are pH-responsive alginate-based hydrogel microparticles incorporating silymarin-loaded PLGA NPs. The obtained data revealed a considerable effect of the alginate content and the drying method onto the characteristics of the prepared alginate-PLGA particles. Also, the developed particles showed promising biodegradability and desirable sustained release profiles of silymarin in addition to enhancing the silymarin overall dissolution.

Acknowledgement

Dr. Stephen Marek, University of Texas at Austin, TX, USA is gratefully acknowledged for helping with the SEM and AFM characterization of the developed particles.

Appendix A. Supplementary data

Supplementary data associated with this article can be found, in the online version, at doi:10.1016/j.carbpol.2010.09.055.

References

Barzaghi, N., Crema, F., Gatti, G., Pifferi, G., & Perucca, E. (1990). Pharmacokinetic studies on IdB 1016, a silybin–phosphatidylcholine complex, in healthy human subjects. *European Journal of Drug Metabolism and Pharmacokinetics*, *15*, 333–338.

Baumann, L. (2005). How to prevent photoaging. *Journal of Investigative Dermatology*, *125*, xii–xiii.

Beckmann-Knopp, S., Rietbrock, S., Weyhenmeyer, R., Böcker, R. H., Beckurts, K. T., Lang, W., et al. (2000). Inhibitory effects of silibinin on cytochrome P-450 enzymes in human liver microsomes. *Pharmacology and Toxicology*, *86*, 250–256.

Bombardelli, E., Spelta, M., Loggia, Della, R., Sosa, S., & Tubaro, A. (1991). Aging skin: Protective effect of silymarin–phytosome. *Fitoterapia*, *62*, 115–122.

Cartiera, M. S., Ferreira, E. C., Caputo, C., Egan, M. E., Caplan, M. J., & Saltzman, M. (2010). Partial correction of cystic fibrosis defects with PLGA nanoparticles encapsulating curcumin. *Molecular Pharmaceutics*, *7*, 86–93.

Chan, L. W., & Heng, P. W. (2002). Effects of aldehydes and methods of cross-linking on properties of calcium alginate microspheres prepared by emulsification. *Biomaterials*, *23*, 1319–1326.

Chen, W., Xia, H., & Wu, W. (2005). Optimized preparation of silymarin dripping pills by a central composite design–response surface method. *Chinese Traditional Herbal Drug*, *36*, 679–683.

El-Sherbiny, I. M. (2010). Enhanced pH-responsive carrier system based on alginate and chemically modified carboxymethyl chitosan for oral delivery of protein drugs: Preparation and *in vitro* assessment. *Carbohydrate Polymers*, *80*, 1125–1136.

El-Sherbiny, I. M., Abdel-Bary, E. M., & Harding, D. R. K. (2010). Preparation and in vitro evaluation of new pH-sensitive hydrogel beads for oral delivery of protein drugs. *Journal of Applied Polymer Science*, *115*, 2828–2837.

Flora, K., Hahn, M., Rosen, H., & Benner, K. (1998). Milk thistle (*Silybum marianum*) for the therapy of liver disease. *The American Journal of Gastroenterology*, *93*, 139–143.

Guenet, J. M. (1992). *Thermoreversible gelation of polymers and biopolymers*. New York: Academic Press., p. 89

Hirano, S., Tsuchida, H., & Nagao, N. (1989). N-acetylation in chitosan and the rate of its enzymic hydrolysis. *Biomaterials*, *10*, 574–576.

Jeong, D. H., Lee, G. P., Jeong, W. I., Do, S. H., Yang, H. J., Yuan, D. W., et al. (2005). Alterations of mast cells and TGF-beta1 on the silymarin treatment for CCl4-induced hepatic fibrosis. *World Journal of Gastroenterology*, *11*, 1141–1148.

Jain, R. A. (2000). The manufacturing techniques of various drug loaded biodegradable poly(lactide-co-glycolide) (PLGA) devices. *Biomaterials*, *21*, 2475–2490.

Jia, J. D., Bauer, M., Cho, J. J., Ruehl, M., Milani, S., Boigk, G., et al. (2001). Antifibrotic effect of silymarin in rat secondary biliary fobrosis is mediated by downregulation of procollagen alphal(I)and TIMP-1. *Journal of Hepatology*, *35*, 392–398.

Kang, J. S., Jeon, Y. J., Park, S. K., Yang, K. H., & Kim, H. M. (2004). Protection against lipopolysaccharide-induced sepsis and inhibition of interleukin-1β and prostaglandin E2 synthesis by silymarin. *Biochemical Pharmacology*, *67*, 175–181.

Kim, N. C., Graf, T. N., Sparacino, C. M., Wani, M. C., & Wall, M. E. (2003). Complete isolation and characterization of silybins and isosilybins from milk thistle (*Silybum marianum*). *Organic Biomolecular Chemistry*, *1*, 1684–1689.

Lahiri-Chatterjee, M., Katiyar, S. K., Mohan, R. R., & Agarwal, R. (1999). A flavonoid antioxidant, silymarin, affords exceptionally high protection against tumor promotion in the SENCAR mouse skin tumorigenesis model. *Cancer Research*, *59*, 622–632.

Liu, D. Z., Chen, W. P., Lee, C. P., Wu, S. L., Wang, Y. C., & Chung, T. W. (2004). Effects of alginate coated on PLGA microspheres for delivery tetracycline hydrochloride to periodontal pockets. *Journal of Microencapsulation*, *21*, 643–652.

Liu, X., Paul, W. S. H., Li, Q., & Chan, L. W. (2006). Novel polymeric microspheres containing norcantharidin for chemoembolization. *Journal of Controlled Release*, *116*, 35–41.

Luper, S. (1998). A review of plants used in the treatment of liver disease: Part 1. *Alternative Medicine Review*, *3*, 410–421.

Matsuda, T., Ferreri, K., Todorov, I., Kuroda, Y., Smith, C. V., Kandeel, F., et al. (2005). Silymarin protects pancreatic beta-cells against cytokine-mediated toxicity: Implication of c-Jun NH_2-terminal kinase and janus kinase/signal transducer and activator of transcription pathways. *Endocrinology*, *146*, 175–185.

Morazzoni, P., & Bombardelli, E. (1995). *Silybum marianum* (Carduus marianus). *Fitoterapia*, *46*, 3–42.

Murata, Y., Kodama, Y., Isobe, T., Kofuji, K., & Kawashima, S. (2009). Drug release profile from calcium-induced alginate–phosphate composite gel beads. *International Journal of Polymer Science*, 1–4.

O'Hara, M. A., Kiefer, D., Farrell, K., & Kemper, K. (1998). A review of 12 commonly used medicinal herbs. *Archives of Family Medicine*, *7*, 523–536.

Ortega-Rivas, E. (2005). Handling and processing of food powders and particulates. In C. Onwulata (Ed.), *Encapsulated and powdered foods* (pp. 78–81). Boca Raton: CRC Press, Taylor & Francis G.

Pepping, J. (1999). Milk thistle: *Silybum marianum*. *American Journal of Health-System Pharmacy*, *56*, 1195–1197.

Schandalik, R., Gatti, G., & Perucca, E. (1992). Pharmacokinetics of silybin in bile following administration of silipide and silymarin in cholecystectomy patients. *Arzneimittelforschung*, *42*, 964–968.

Sheu, S. Y., Lai, C. H., & Chiang, H. C. (1998). Inhibition of xanthine oxidase by purpurogallin and silymarin group. *Anticancer Research*, *18*, 263–267.

Sonnenbichler, J., Scalera, F., Sonnenbichler, I., & Weyhenmeyer, R. (1999). Stimulatory effects of silibinin and silicristin from the milk thistle *Silybum marianum* on kidney cells. *Journal of Pharmacology and Experimental Therapeutics*, *290*, 1375–1383.

Sonnenbichler, J., & Zetl, I. (1986). Biochemical effects of the flavanolignane silibinin on RNA, protein and DNA synthesis in rat livers. In V. Cody, E. Middleton, & J. B. Harbourne (Eds.), *plant flavonoids in biology and medicine: Biochemical, pharmacological, and structure-activity relationships* (p. 319). New York: Alan, R. Liss.

Trubetskoy, V. S. (1999). Polymeric micelles as carriers of diagnostic agents. *Advanced Drug Delivery Reviews*, *37*, 81–88.

Wu, W., Wang, Y., & Que, L. (2006). Enhanced bioavailability of silymarin by self-microemulsifying drug delivery system. *European Journal of Pharmaceutics and Biopharmaceutics*, *63*, 288–294.

Zahoor, A., Sharma, S., & Khuller, G. K. (2005). Inhalable alginate nanoparticles as antitubercular drug carriers against experimental tuberculosis. *International Journal of Antimicrobial Agents*, *26*, 298–303.

Zi, X., Feyes, D. K., & Agarwal, R. (1998). Anticarcinogenic effect of a flavonoid antioxidant, silymarin, in human breast cancer cells MDA-MB 468: Induction of G1 arrest through an increase in Cip1/p21 concomitant with a decrease in kinase activity of cyclin-dependent kinases and associated cyclins. *Clinical Cancer Research*, *4*, 1055–1064.

Zi, X., Grasso, A. W., Kung, H. J., & Agarwal, R. (1998). A flavonoid antioxidant, silymarin, inhibits activation of erbB1 signaling and induces cyclin-dependent kinase inhibitors, G1 arrest, and anticarcinogenic effects in human prostate carcinoma DU145 cells. *Cancer Research*, *58*, 1920–1929.